

The Annealing-Induced Shape Deformation of Hydrothermal-Grown ZnO Nanorods

This article has been downloaded from IOPscience. Please scroll down to see the full text article.

2012 Chinese Phys. Lett. 29 017804

(<http://iopscience.iop.org/0256-307X/29/1/017804>)

View [the table of contents for this issue](#), or go to the [journal homepage](#) for more

Download details:

IP Address: 159.226.165.151

The article was downloaded on 05/09/2012 at 06:10

Please note that [terms and conditions apply](#).

The Annealing-Induced Shape Deformation of Hydrothermal-Grown ZnO Nanorods *

ZHENG Zhong-Kui(郑仲飏)¹, DUANMU Qing-Duo(端木庆铎)^{1**}, ZHAO Dong-Xu(赵东旭)^{2**},
WANG Li-Dan(王丽丹)², SHEN De-Zhen(申德振)²

¹School of Science, Changchun University of Science and Technology, Changchun 130022

²Key Laboratory of Excited State Processes, and Changchun Institute of Optics, Fine Mechanics and Physics, Chinese Academy of Sciences, Changchun 130033

(Received 28 September 2011)

The shape deformation of hydrothermal-grown ZnO nanorods is observed. After annealing at high temperature, hexagonal ZnO nanorods change to become cylinder-like ones. The adjacent nanorods tend to connect to each other to form one nanostructure. Photoluminescence measurements show that a sample annealed at 600°C has a strong ultraviolet emission with a very weak visible emission, and with increasing annealing temperature the visible emission becomes more intense. It can be concluded from analyses of the morphological changes that the surface reaction between the doped C and ZnO is the main reason for the shape deformation of the ZnO nanorods.

PACS: 78.67.-n, 78.67.Qa

DOI:10.1088/0256-307X/29/1/017804

As a wide bandgap semiconductor, ZnO nanostructures are a promising candidate for electronic and optoelectronic applications at the nanoscale.^[1–3] Generally, materials of reduced size demonstrate melting points lower than those of their bulk forms. Because the melting point of bulk ZnO is as high as 1750°C, ZnO shows good thermal stability,^[4–7] and the growth temperature for single crystalline ZnO thin films reaches 700–900°C. By the physical vapor transport method, one-dimensional (1D) ZnO nanostructures could be obtained with a growth temperature above 900°C.^[8] However, some researchers recently reported that the melting point of ZnO nanorods grown by thermal decomposition or the hydrothermal method could be decreased to 600–700°C.^[4] The diameters of these nanorods can be 10 nm to several tens of nanometers, and a morphological change in the ZnO nanostructures annealed at high temperature was reported, which was ascribed to the melting point decrease for the nano-sized ZnO.^[9] Some theoretical works have also shown that the size and shape of ZnO nanostructures can affect the melting temperature T_m .^[9,10] Moreover, the melting of materials normally induces structural and property changes, which is a major concern in applications. Therefore, it is of great interest to study the melting behavior and the induced structural and property changes of nano-sized materials.

In nano- and micro-electronics, the thermal behavior of active components is an important factor affecting the reliability of these devices.^[11–14] It is there-

fore important to understand the thermal stability of ZnO nanostructures. In this study, we fabricate ZnO nanorods using the hydrothermal method. With annealing of the sample at different temperatures, the structural and photoluminescent (PL) properties are examined.

A ZnO seed layer with a thickness of 100 nm in the (002) orientation was deposited on an Si substrate by the magnetron sputtering method using a 99.99% ZnO target. The ZnO nanorods were grown on the ZnO seed layer/Si substrate by a hydrothermal method. Zinc acetate $[\text{Zn}(\text{CH}_3\text{COO})_2 \cdot 2\text{H}_2\text{O}]$ and hexamethylenetetramine ($\text{C}_6\text{H}_{12}\text{N}_4$) were used as the reactant sources. We dissolved 0.02 M $[\text{Zn}(\text{CH}_3\text{COO})_2 \cdot 2\text{H}_2\text{O}]$ and 0.02 M $\text{C}_6\text{H}_{12}\text{N}_4$ in de-ionized water to form a 50 mL solution. Then, a 30 mL solution was moved to a reaction kettle with a 50 mL capacity. The ZnO seeding layer/Si substrate was put into the solution, and the reaction kettle was preserved at 90°C for 16 h. After the reaction, the samples were taken out of the reaction kettle, cleaned with de-ionized water and dried in air at 60°C for 2 h. Finally, the samples were annealed in air at different temperatures of 600, 700, 800, 900 and 1000°C for 30 min, respectively.

All the as-grown and annealed samples were characterized by field-emission scanning electron microscopy using a Hitachi S4800 microscope, and energy-dispersive x-ray spectroscopy (EDS, GENE SIS 2000 XMS 60S, EDAX, Inc.) attached to the SEM. The crystal structures of the samples were de-

*Supported by the National Basic Research Program of China under Grant No 2011CB302004, the Innovation Project of the Chinese Academy of Sciences under Grant No KJJCX2-YW-W25, and the National Natural Science Foundation of China under Grant Nos 60506014 and 10974197.

**Corresponding authors. Email: duanmu@cust.edu.cn; dxzhao2000@yahoo.com.cn

© 2012 Chinese Physical Society and IOP Publishing Ltd

terminated by x-ray diffraction (XRD, D/max-RA) using Cu K α radiation with an area detector. Photoluminescence (PL, LABRM-UV Jobin Yvon) measurements were performed using a He-Cd laser operating at 325 nm as the excitation source.

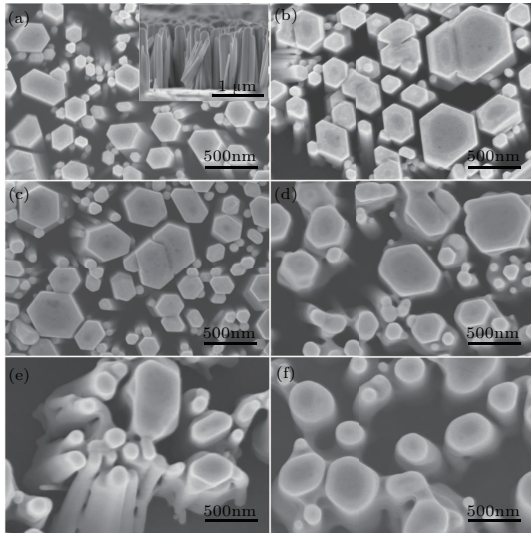


Fig. 1. SEM images of as-grown ZnO nanorods (a), and annealed at 600 (b), 700 (c), 800 (d), 900 (e) and 1000°C (f) for 30 min. The inserted image shows the corresponding cross-sectional SEM image for the as-grown ZnO nanorods.

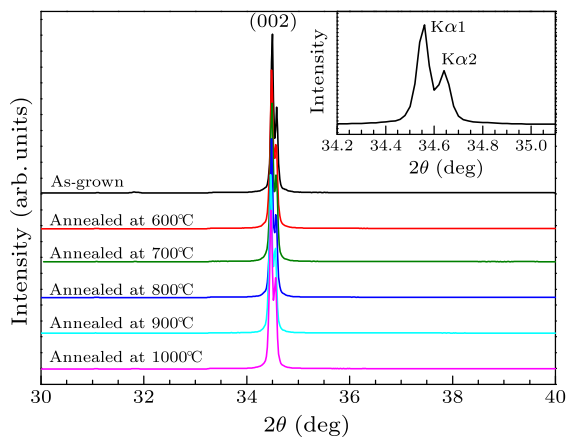


Fig. 2. The x-ray diffraction patterns for ZnO nanorods that were as-grown and at different annealing temperatures. The inset shows the amplified patterns of the as-grown ZnO nanorods.

The morphologies of the as-grown and annealed ZnO samples are shown in Fig. 1. The as-grown sample (Fig. 1(a)) is composed of straight and hexagonal-shaped nanorods with different diameters ranging from 80 to 300 nm. The inserted image shows that the corresponding cross-sectional SEM image for the as-grown ZnO nanorods is about 1 μ m in length. At low annealing temperatures of 600 and 700°C, ZnO nanorods keep a hexagonal structure without any changes, as shown in Fig. 1(b) and (c). However, with the annealing temperature increasing to 800°C, two

obvious changes could be observed in Fig. 1(d). First, the adjacent nanorods tend to connect to each other, designated by the white circle. Second, each angle of the tops of the hexagonal become less sharp. These two characteristics are much clearer with a further increase in the annealing temperature to 900 and 1000°C (Fig. 1(e) and (f)). At 1000°C the hexagonal-shaped nanorods are completely changed into cylinder-like nanorods. The adjacent nanorods then combine together to form a whole one (Fig. 1(f)).

Figure 2 shows the XRD curves of ZnO nanorods under different annealing temperatures. For all the samples, the positions of the diffractive peaks in the XRD curves are the same. All the diffraction peaks originate from the ZnO wurtzite structure, with lattice parameters of $a = 0.325$ and $c = 0.521$ nm. The strong ZnO (002) diffraction peak indicates that the samples are of c -axis orientation. The full width at half maximum (FWHM) of the sharp (002) diffraction peak for all the samples is only 0.11–0.12°. The inset shows the amplified patterns of the as-grown ZnO nanorods, with the two peaks located at 34.43 and 34.52° from the K α_1 and K α_2 diffractions. The XRD results indicate that after annealing, the crystalline structure does not change.

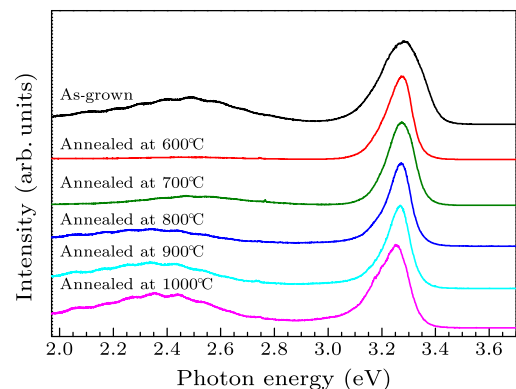


Fig. 3. The PL spectrum of the as-grown ZnO nanorods and those at different annealing temperatures, measured at room temperature.

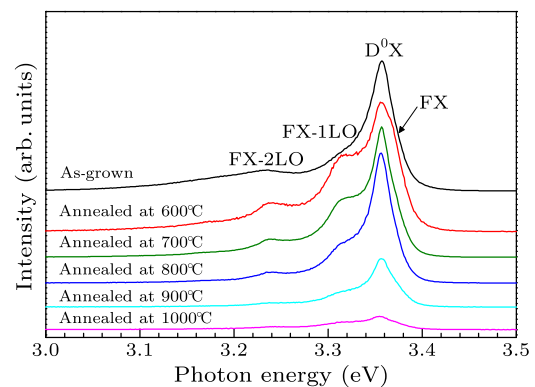


Fig. 4. The PL spectrum of the as-grown ZnO nanorods and those at different annealing temperatures, measured at 83 K.

To study the effect of annealing on the PL emission, PL spectra were measured using a He-Cd laser at 325 nm as an excitation source, as shown in Fig. 3. The PL spectrum of the as-grown ZnO nanorods consists of a UV emission and a deep-level emission. The UV emission could be attributed to the exciton recombination-related near-band edge emission in ZnO. The deep-level emission is mainly ascribed to oxygen vacancies.^[15] For the sample annealed at 600°C, the visible emission is completely quenched. Only a strong UV emission with a narrow FWHM could be observed. The deep-level related emission appears at 700°C and becomes stronger with a further increase in the annealing temperature, which indicates the evaporation of the O atoms to generate more O vacancies in ZnO. There is a competing process between the O atoms getting into the lattice and the thermal evaporation out of the ZnO lattice in atmosphere.^[16] At low annealing temperatures (600°C), the adsorption rate of the O atoms is faster than that of the escaping ones. Hence, more O atoms can compensate for the O vacancies at lower annealing temperatures, resulting in the weakening of the visible PL emission. However, at high annealing temperatures (700–1000°C), the escape rate of the O atoms becomes larger than the adsorption rate, which leads to the formation of more O vacancies in the ZnO lattice.

To further understand the origin of the PL emissions in ZnO nanorods, low-temperature PL measurements were performed at 83 K as shown in Fig. 4. The PL spectra from all the samples are dominated by the neutral donor bound exciton (D^0X) emission located at 3.358 eV, with two weak emission peaks located at 3.310 and 3.236 eV, which are attributed to the first-order and second-order LO-phonon replicas of the free exciton emission (FX-1LO and FX-2LO).^[17] For the samples annealed at 600°C, a weak free exciton (FX) emission located at 3.370 eV could be observed. The FX-1LO and FX-2LO peaks become more sharp at an annealing temperature of 600°C. However, with an increase in the annealing temperature, the sharp transitions develop into a broad band. The intensity of the D^0X emission decreases more slowly than that of the FX-1LO and FX-2LO, and gradually, the FX-1LO and FX-2LO peaks merge into the low-energy tail of the D^0X peak.

According to the study carried out by Guisbiers *et al.*, the T_m of ZnO nanowires with a radius of 5 nm and a length of 100 nm is about 1430°C, which is much lower than the bulk one.^[9] However, based on our data, this explanation is not appropriate due to the following reasons. First, the diameters of our ZnO nanowires are in the range 80–300 nm. In this value, the size effect is so weak that the physical properties of the nanowires are almost the same as the bulk ones. Second, the melting process leads to a phase change

from the solid state to the liquid one, resulting in the great shape change. However, in our result with the increasing annealing temperature from 600 to 1000°C, the nanostructures keep the 1D shapes and the diameters are not decreased by too much. Referring to the physical transfer method, the ZnO nanostructures grown at high temperature (950°C) are still of a hexagonal shape. Therefore, we attribute the shape deformation in our experiment to the surface reaction in ZnO nanorods.

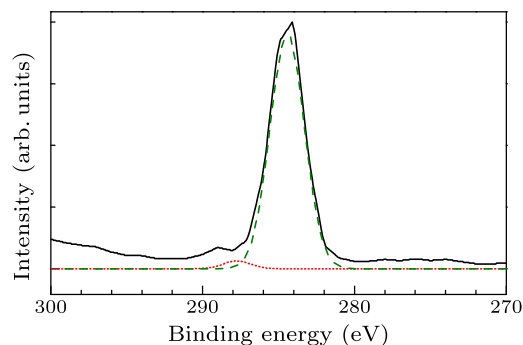


Fig. 5. The XPS spectrum of the annealed ZnO nanorods.

When the contents of the elements in the ZnO nanostructures were analyzed, C could be detected, as shown in the x-ray photoelectron spectrum (Fig. 5), which may be due to the C doping into ZnO during the growth process. Based on the XRD and PL spectra, the doping does not affect the structural and luminescent properties. By Gauss fitting, two binding energy peaks located at 284 and 288 eV could be obtained, which correspond to the C–H and C–O bonds. With an increase in the annealing temperature, the C could react with the ZnO to form CO and Zn vapors, like a carbothermal method (above 800°C). Then the vapors react again to grow ZnO. Because of the above process, shape deformation occurs and the adjacent nanorods can be connected, and due to the escape of oxygen from the ZnO nanorods, this process could generate more oxygen vacancies in ZnO. The emission intensity of the visible band increases with enhancing annealing temperature.

In conclusion, hydrothermal-grown ZnO nanorods only show good thermal stability under annealing temperatures below 600°C. At high annealing temperatures, the morphology of the ZnO nanorods changes greatly. At 1000°C the hexagonal-shaped nanorods are completely changed into cylinder-like ones, and the adjacent nanorods are combined together to form a whole one. We attributed the shape deformation to the surface reaction in the ZnO nanorods.

References

- [1] Ozgur U, Alivov Y I, Liu C, Teke A, Reshchikov M A, Do-

- gan S, Avrutin V, Cho S J and Morkoc H 2005 *J. Appl. Phys.* **98** 041301
- [2] Wang Z L 2004 *J. Phys.: Condens. Matter* **16** R829
- [3] Lieber C M and Wang Z L 2007 *Mater. Res. Soc. Bull.* **32** 99
- [4] Yan Z J, Zhu K and Chen W P 2008 *Appl. Phys. Lett.* **92** 241912
- [5] Huang M H, Mao S, Feick H, Yan H, Wu Y Y, Kind H, Weber E, Russo and Yang P D 2001 *Science* **292** 1897
- [6] Chik H, Liang J, Cloutier S G, Kouklin N and Xu J M 2004 *Appl. Phys. Lett.* **84** 3376
- [7] Lao C S, Paik M C, Kuang Q, Deng Y L, Sood A K, Polla D L and Wang Z L 2007 *J. Am. Chem. Soc.* **129** 12096
- [8] Fang F, Zhao D X, Zhang J Y, Shen D Z, Lu Y M, Fan X W, Li B H and Wang X H 2007 *Nanotechnology* **18** 235604
- [9] Guisbiers G and Pereria S 2007 *Nanotechnology* **18** 435710
- [10] Su X, Zhang J Y and Zhu M M 2006 *Appl. Phys. Lett.* **88** 061913
- [11] Lu W and Lieber C M 2006 *J. Phys. D: Appl. Phys.* **39** R387
- [12] Zhou W, Yang J, Xia S J, Li X and Tang W 2011 *Chin. Phys. Lett.* **28** 117801
- [13] Yoon Y, Lin J S, Pearton S J and Guo J 2007 *J. Appl. Phys.* **101** 024301
- [14] Yang C, Zhang G, Lee D Y, Li H M, Lim Y D, Yoo W J, Park Y J and Kim J M 2011 *Chin. Phys. Lett.* **28** 035202
- [15] Wei X Q, Zhang Z G, Liu M, Chen C S, Sun G, Xue C s, Zhuang H Z and Man B Y 2007 *Mater. Chem. Phys.* **101** 285
- [16] Meng X Q, Shen D Z, Zhang J Y, Zhao D X, Lu Y M, Dong L, Zhang Z Z, Liu Y C and Fan X W 2005 *Solid State Commun.* **135** 179
- [17] Fang F, Zhao D X, Li B H, Zhang J Y, Shen D Z and Wang X H 2010 *J. Phys. Chem. C* **114** 12477